

Mechanisms and Machine Science

Giuseppe Carbone
Med Amine Laribi *Editors*

Advances in Automation, Mechanical and Design Engineering


SAMDE 2023



 Springer

The Springer logo, which consists of a white chess knight icon on a red background, followed by the word "Springer" in a white serif font.

Series Editor

Marco Ceccarelli , *Department of Industrial Engineering, University of Rome Tor Vergata, Roma, Italy*


Advisory Editors

Burkhard Corves, *RWTH Aachen University, Aachen, Germany*

Victor Glazunov, *Mechanical Engineering Research Institute, Moscow, Russia*

Alfonso Hernández, *University of the Basque Country, Bilbao, Spain*

Tian Huang, *Tianjin University, Tianjin, China*

Juan Carlos Jauregui Correa , *Universidad Autonoma de Queretaro, Queretaro, Mexico*

Yukio Takeda, *Tokyo Institute of Technology, Tokyo, Japan*

Sunil K. Agrawal, *Department of Mechanical Engineering, Columbia University, New York, NY, USA*

This book series establishes a well-defined forum for monographs, edited Books, and proceedings on mechanical engineering with particular emphasis on MMS (Mechanism and Machine Science). The final goal is the publication of research that shows the development of mechanical engineering and particularly MMS in all technical aspects, even in very recent assessments. Published works share an approach by which technical details and formulation are discussed, and discuss modern formalisms with the aim to circulate research and technical achievements for use in professional, research, academic, and teaching activities.

This technical approach is an essential characteristic of the series. By discussing technical details and formulations in terms of modern formalisms, the possibility is created not only to show technical developments but also to explain achievements for technical teaching and research activity today and for the future.

The book series is intended to collect technical views on developments of the broad field of MMS in a unique frame that can be seen in its totality as an Encyclopaedia of MMS but with the additional purpose of archiving and teaching MMS achievements. Therefore, the book series will be of use not only for researchers and teachers in Mechanical Engineering but also for professionals and students for their formation and future work.

The series is promoted under the auspices of International Federation for the Promotion of Mechanism and Machine Science (IFToMM).

Prospective authors and editors can contact Mr. Pierpaolo Riva (publishing editor, Springer) at: pierpaolo.riva@springer.com

Indexed by SCOPUS and Google Scholar.


Giuseppe Carbone · Med Amine Laribi
Editors

Advances in Automation, Mechanical and Design Engineering

SAMDE 2023

 Springer

Editors

Giuseppe Carbone 
DIMEG
University of Calabria
Rende, Italy

Med Amine Laribi
SP2MI—Site du Futuroscope
University of Poitiers
Poitiers, France

ISSN 2211-0984

ISSN 2211-0992 (electronic)

Mechanisms and Machine Science

ISBN 978-3-031-62663-0

ISBN 978-3-031-62664-7 (eBook)

<https://doi.org/10.1007/978-3-031-62664-7>

© The Editor(s) (if applicable) and The Author(s), under exclusive license
to Springer Nature Switzerland AG 2024

This work is subject to copyright. All rights are solely and exclusively licensed by the Publisher, whether the whole or part of the material is concerned, specifically the rights of translation, reprinting, reuse of illustrations, recitation, broadcasting, reproduction on microfilms or in any other physical way, and transmission or information storage and retrieval, electronic adaptation, computer software, or by similar or dissimilar methodology now known or hereafter developed.

The use of general descriptive names, registered names, trademarks, service marks, etc. in this publication does not imply, even in the absence of a specific statement, that such names are exempt from the relevant protective laws and regulations and therefore free for general use.

The publisher, the authors and the editors are safe to assume that the advice and information in this book are believed to be true and accurate at the date of publication. Neither the publisher nor the authors or the editors give a warranty, expressed or implied, with respect to the material contained herein or for any errors or omissions that may have been made. The publisher remains neutral with regard to jurisdictional claims in published maps and institutional affiliations.

This Springer imprint is published by the registered company Springer Nature Switzerland AG
The registered company address is: Gewerbestrasse 11, 6330 Cham, Switzerland

If disposing of this product, please recycle the paper.

Preface

We are pleased to present the preface for the proceedings of the 4th International Symposium on Automation, Mechanical and Design Engineering (SAMDE 2023), held from 8th to 10th December 2023 in Nanjing, China, and organized by Nanjing University of Aeronautics and Astronautics, with co-organization by Dalian University. SAMDE 2023 garnered an enthusiastic response, receiving a total of 108 paper submissions. Following a rigorous review process, 50 papers were selected for inclusion in this volume, highlighting the quality and relevance of the research presented. Covering diverse topics such as robotics, intelligent manufacturing, process control and automation, precision and ultra-precision machining, mechanism and machine design, as well as advanced materials and structures, these papers represent the forefront of innovation and scholarship in the fields of automation, mechanical and design engineering.

The symposium featured esteemed keynote speakers who shared their insights and expertise with attendees. Prof. Xingjian Jing from City University of Hong Kong, China, offered valuable knowledge in the field, while Prof. Ramesh K. Agarwal from Washington University, USA, and Prof. Giuseppe Carbone from the University of Calabria, Italy, contributed significantly to the event.

The discussions, presentations and networking opportunities at SAMDE 2023 were invaluable, fostering collaboration and innovation in automation, mechanical and design engineering. We extend our sincere gratitude to all participants, organizers, reviewers and speakers for their invaluable contributions to making this symposium a resounding success.

This book showcases the culmination of research and discussions presented during the symposium. As we present this compilation of proceedings, we eagerly anticipate the opportunity to welcome future editions of SAMDE, with the aim of building upon the success of this year's conference and further enhancing collaborations and innovations in the automation, mechanical and design engineering field.

We take the opportunity to express our gratitude to Anna H. M. Wong, Conference Managing Director who made significant efforts for the smooth running of SAMDE 2023 Conference and for the successful completion of this book. Likewise, we express our gratitude to all the members of the conference committees for their valuable support and contributions.

Giuseppe Carbone
Med Amine Laribi

Amir Zare Shahneh	Cranfield University, UK
Pavlo Maruschak	Ternopil Ivan Pul'uj National Technical University, Ukraine
Hamid Reza Karimi	Politecnico di Milano, Italy
Frank Werner	Otto von Guericke University Magdeburg, Germany
Guennadi Kouzaev	Norwegian University of Science and Technology, Norway
Adrian Olaru	University Politehnica of Bucharest, Romania
Chechina Natalia	Bournemouth University, UK
Alessandro Casavola	Università della Calabria, Italy

Asia

Quanxin Zhu	Hunan Normal University, China
Xie Ming	Nanyang Technological University, Singapore
Md. Akhtaruzzaman	The National University of Malaysia, Malaysia
Walter Nsengiyumva	Fuzhou University, China
Shanling Dong	Zhejiang University, China
Chong Zhi Lin	Universiti Tunku Abdul Rahman, Malaysia
Md. Hazrat Ali	Nazarbayev University, Kazakhstan
Fan Gao	Chongqing Chuanyi Automation Co., Ltd., China
Debdulal Das	Indian Institute of Engineering Science and Technology, India
Guanglei Wu	Dalian University of Technology, China
Ali El-Zaart	Beirut Arab University, Lebanon
Alpay Tamer Erturk	Kocaeli University, Turkey
Tang Sai Hong	University Putra Malaysia, Malaysia
Shaw Voon Wong	University Putra Malaysia, Malaysia
Anand J. Kulkarni	MIT World Peace University, India
Boon Giin Lee	University of Nottingham Ningbo China, China
Mehmet Serdar Guzeli	Ankara Üniversitesi, Turkey
Jianfeng Ren	University of Nottingham Ningbo China, China
Huseyin Canbolat	Ankara Yıldırım Beyazıt University, Turkey
Shunli Wang	Southwest University of Science and Technology, China
Hao Sun	Nankai University, China
Zhaohua Liu	Hunan University of Science and Technology, China
Bing Wang	Fuzhou University, China
Jawaid Daudpoto	Mehran University of Engineering and Technology, Pakistan

Mohammad Yeakub Ali	International Islamic University Malaysia, Malaysia
Anshuman Srivastava	SIET Allahabad, India
Norhazilan Md. Noor	Universiti Teknologi Malaysia, Malaysia
Nazir Ahmad Zafar	COMSATS Institute of Information Technology, Pakistan
Christos Spitas	Nazarbayev University, Kazakhstan
Syed Bahari Ramadan Bin Syed Adnan	University of Malaya, Malaysia
Muhamad Mat Noor	Universiti Malaysia Pahang, Malaysia
Volodymyr Brazhenko	Zhejiang Normal University, China
Cheng Siong Chin	Newcastle University, Singapore
Ryspek Usubamatov	Kyrgyz State Technical University, Kyrgyzstan
Dirman Hanafi	Universiti Tun Hussein Onn Malaysia (UTHM), Malaysia
Chai Shijie	Nanyang Technological University, Singapore
Bin Zhao	Xidian University, China
Elammaran Jayamani	Swinburne University of Technology Sarawak Campus, Malaysia
Puzhao Zhang	Xidian University, China
Mohd Amri Lajis	Universiti Tun Hussein Onn Malaysia (UTHM), Malaysia
Aidy Ali	National Defence University of Malaysia, Malaysia
Mohd Ashraf Bin Ahmad	University Malaysia Pahang, Malaysia
Chien-Chih Wang	Ming Chi University of Technology, Taiwan
Tianjiao An	Changchun University of Technology, China
Mohd Faisal Bin Hushim	Universiti Tun Hussein Onn Malaysia, Malaysia

Oceania

Tao Huang	James Cook University, Australia
Abbas Amini	Western Sydney University, Australia
Ibrahim Sultan	Engineering and IT Federation University, Australia

Africa

Mohamed Arezki Mellal	Hamed Bougara University (UMBB), Algeria
Guelailia Ahmed	Algerian Space Agency, Algeria
Yousef Moh. Abueejela	College of Electronic Technology, Libya

Contents

Robotics

Modeling and Simulation of a Slung Load System for UAS	3
<i>Jacob Juul Naundrup, Denys Grombacher, Jan Dimon Bendtsen, and Anders la Cour-Harbo</i>	
Research on Posture-Dependent Mode Coupling Chatter in Robotic Milling ...	13
<i>Ming Ma, Xiong Huang, Tao Wu, Cencen Yang, and Lin Zhou</i>	
Design of Intelligent Anti-theft Alarm System for Electric Bicycles Based on NB-IoT	23
<i>Qiao Tan, Guanghong Xu, and Junnan Zhu</i>	
On Necessity of Conscious Learning: From Robots to Humans	33
<i>Juyang Weng</i>	
High-Precision Tracking Simulation of Stepper Motor Based on Improved SVPWM	56
<i>Wenrui Gao, Huimin Cui, and Kuiying Yin</i>	
Research on Air Autonomous Route Re-planning Technology of Combat Aircraft	66
<i>Chun-xia Yin and Tao Chu</i>	
Research on Fault Prediction of Electric Spindle in Five-Axis Machining Center Based on Bayes-SVM	73
<i>Shuo Wang, Zhenliang Yu, Wenwu Zhang, and Jian Zhang</i>	
Innovative Design of an Upper Limb Passive Exoskeleton for Electrical Work: A Preliminary Exploration	80
<i>Jianzhong Wang, Zhenghua Dong, Junfang Zheng, Dongwei Zhao, Lang Shen, Shouqian Sun, Xuequn Zhang, Guoxian Xu, and Kaiyuan Zhang</i>	
Emergency Robotic System for the Elderly Behavior Detection	95
<i>Jingyi Tao, Xiaorui Mo, Hao Wen, Chuyuan Luo, Zheng Wang, and Banggui Zheng</i>	

Intelligent Manufacturing

Development of Actuator Based on IMC Core Module 109
Yong Luo, Ling Feng, and Biyan Pi

Development of FF Bus Temperature Transmitter Based on IMC 121
Kean Zhao, Xiaobo Zhong, and Liangrong Ma

Structural Design and Research of Bionic Turtle Underwater Surveyor 130
Xiao Han and Siyang Zhang

Structural Design and Research of Turtle Paddling Sports Model 137
Xiao Han and Siyang Zhang

Towards a Unified Theory on the Superposition Principles 143
Xiayu Chen, Bing Wang, Chenmin Zhao, Dongmei Du, Chenglong Guan, and Shuncong Zhong

Preliminary Research and Evaluation on Civil Aircraft Flight Test Management System 151
Fei Ma and Lisu Liu

Research on BO-CNN Based Tool Wear Status Monitoring Method 160
Shuo Wang, Zhenliang Yu, Jian Zhang, Liyao Zhou, and Wenwu Zhang

Research on Quasi-real-time Flight Test Data Identification Method and Software Development 167
Wu Jiang

Process Control and Automation

Control-Based Continuation Methods for Bifurcation Characteristic Study of Landing Gear Strut Locking Mechanism 177
Yangyang Li, Yin Yin, Zhipeng Zhang, Shengxiao Wu, Xiaohui Wei, and Hong Nie

FEM Analyses of Excitation Efficiency of Airborne Ultrasound Catalysis Mechanisms 186
Zongheng Xiang and Junhui Hu

Research on Multi-model Hierarchical Optimization Design Technology for Railway Body Structure 193
Liang Chang, Lilong Luo, Xiaohua Nie, and Wenjie Guo

Vehicle Positioning Method in GNSS-Denied Environment:
INS/ODO/Mag Integrated Navigation System Algorithm 202
*Jia Tian, Hui Luo, Shiyuan Zhou, Zhihe Chen, Kaixin Luo,
and Bainan Yang*

Research on the Concept of Missile Cooperative Combat 214
Wei Pan, Chi Zhang, Tianhui Wang, Ming Liang, and Gang Wang

Adaptive Sliding Mode Control of Magazine Based on Fuzzy Theory 222
Pengyao Bai, Longmiao Chen, and Quan Zou

Research on the Load-Sensitive Feed Speed Regulating Hydraulic System
of the Drilling Robot 231
Hang Chen and Xiaohua Liu

Numerical Simulation of One-Dimensional Barrier Penetration 240
Xingrong Zheng, Yujie Li, and Kaiqiang Xie

Analysis of Interference Factors on Paralleling Multi-satellite Separation 247
*Yuqin Zeng, Changzheng Xiang, Wenfeng Dong, Xiyang Wei,
Ziyao Dai, Qisheng Zhang, and Libo Wang*

Study on the Influence of AC Power Supply Frequency on Electric Load 254
Ying Liu

Precision and Ultra-Precision Machining

Experimental Study on the Design of Impedance Vibration Reduction
Inserts and Aluminum Alloy Cutting for Milling Robots 263
Shuai Li and Guimei Lv

Optimization Study of Heating Structure Based on the Temperature
Uniformity of Mold Cavity 270
Zhiyin Xie, Zhonggui Xu, Yingru Li, Shidong Li, Linli Tan, and Liu Qin

Research on Laser On-Line Monitoring for Counter-Roller Spinning
of Thin-Walled Cylindrical Parts 278
Fan Li, Xue-wen Cao, and Sheng-dun Zhao

Study on Material Properties of Protective Clothing in High Temperature
Operation 288
Feifei Li, Yibin Dong, Jiaqi Guo, Jian Zhao, and Xingrong Zheng

Research on Optimal Design of Cutting Edge of Shear Machine Based
on LS-DYNA 295
Meili Yu and Shaohei Dai

An Experimental and Simulation Study on Machining Damage of T-800
CFRP Multi-edge Milling Process 303
*Yiqi Wang, Zhiqiang Cheng, Wanyue Song, Bochuan Liu,
and Liangzi Chen*

Mechanism and Machine Design

Application of GPS Technology in Missile Measurement and Control 313
Wei Pan, Chi Zhang, Tianhui Wang, Ming Liang, and Tang Tong

The Mechanism of Formability Improvement in Multi-pass Incremental
Flanging 318
Chong Tian and Da-Wei Zhang

Analysis of Failure in Corrugated Metal Pipe Under Acid Pickling Due
to Grain Boundary Cracking 325
Xinlang Zuo, Hao He, Guoqing Guo, Huanyu Zhao, and Xiaotong Guo

Research on Flight Test Technologies of FMS Vertical Profile for Civil
Aircraft 332
Xin Li

Research and Application of Expansion Deformation Mechanism
of Six-Row Rolling Linear Guide Pair 339
Guangyu Zhai, Fei Yang, Changguang Zhou, and Hutian Feng

Advanced Materials and Structures

An Ultrasonic Cooling Method for Small Solid Heat Sources 353
Shuo Zhang and Junhui Hu

Synthesis and Characterization of Porous NiCo-LDH Nanosheets
for Room-Temperature H₂S Gas Sensor 359
Qiuxia Ma and Junhui Hu

Elasto-Plastic FEM Analysis of Alternating Rock Mass Based by Cosserat
Constitutive Model and Its Numerical Simulation 365
*Jiancheng Zhang, Xueguo Jiang, Zikang Jia, Maosen Cao,
Ziwen Zhang, and Chen Yang*

Synthesis and Mechanical Properties of a 3D Printable Photocurable Resin Composed of Rosin and Triethylene Glycol Dimethacrylate	383
<i>Hanrui Xu, Shijie Huang, Lei Ding, Qiang Li, Jianhui Song, Danyang Sun, Chuanyang Tang, Mengyu Liu, Yan Liu, and Shuoping Chen</i>	
Two-Dimensional CN Material Structure Prediction Based on Machine Learning	391
<i>Longzhou Hu, Anqiu Li, Leiao Fu, Lizhong Sun, Wenjuan Jiang, and Chaogui Tan</i>	
Fatigue Properties of Asphalt Mixtures Using Granite Aggregates	401
<i>Kun Xu, Hao Ma, Salah Saeed Abdo AL-khulaidi, and Peilong Li</i>	
Effect of Al on the Microstructure and Properties of Cu-15Ni-8Sn Alloy	409
<i>Wei Luo, Lijun Peng, Xujun Mi, Haofeng Xie, and Zhen Yang</i>	
The Roles of the Halide Elements and the Drive Mode for the Stability of Blue Perovskite Light-Emitting Diodes	416
<i>Buyue Zhang and Xinyu Chen</i>	
Precursors, Structure and Properties of Carbon Fibers	421
<i>Zhengwei Cui and Guanming Yuan</i>	
Effect of Deformation Temperatures on the Microstructure and Mechanical Properties of a Non-isoatomic AlCoFeMnNi High-Entropy Alloy	432
<i>Mei Li, Mingze Wang, and Yongfeng Shen</i>	
Research of Climb Performance Calculation Method and Program Implementation for Civil Aircraft Flight Test	443
<i>Wu Jiang</i>	
A High-Energy-Density Hybrid Capacitor Enabled by Fibrous PANI and V2O5/MXene	450
<i>Jing He, Shilin Zhou, and Chenxiang Wang</i>	
Author Index	461

Robotics



Modeling and Simulation of a Slung Load System for UAS

Jacob Juul Naundrup¹(✉), Denys Grombacher², Jan Dimon Bendtsen¹,
and Anders la Cour-Harbo¹

¹ Department of Electronic Systems, Aalborg University, Fredrik bajers vej 7C,
9220 Aalborg, Denmark

jnpe@es.aau.dk

² Department of Geoscience, Aarhus University, Aarhus, Denmark

<http://www.aau.dk>

Abstract. Flying UAS with suspended loads poses maneuverability challenges. This paper proposes a novel method to model a slung load system using rigid bodies and lumped parameters, simulating a flexible tether. The aim is to validate different tether configurations for feasibility before field deployment. The simulation incorporates second-order drag for aerodynamic calculations, dependent on Reynolds number and object shape. Implemented in Simulink with Simscape for physical simulation, the model is validated under varied wind velocities and attachment point movements. A 3D model verifies simulation data and enhances safety and efficiency for UAS operations with suspended loads.

Keywords: UAS · Simscape · Lumped-parameters · Slung load

1 Introduction

Non-invasive geophysical imaging presents one of the most cost-efficient solutions for delivering this information [1]. In this work, a geophysical imaging platform called SuperTEM is used; it uses a transient electromagnetic (TEM) system. Briefly, TEM is an inductive measurement capable of imaging spatial/temporal variations in the electrical properties of the subsurface. A system is composed of a transmitter/receiver pair. The transmitter serves to pulse a strong current, which is rapidly shut off to generate eddy currents that circulate at depth. The receiver measures these eddy currents' strength and time dependence, allowing an inversion framework to estimate the electrical resistivities at a depth consistent with collected data.

TEM systems can be ground-based, towed by a vehicle [2], or airborne [3]. Airborne options offer extensive coverage but sacrifice depth resolution and incur higher costs. Ground-based systems provide better depth resolution but cover less area. Drone-based systems bridge this gap, particularly useful in challenging terrains. This work proposes a semi-airborne system with a ground-based

Thanks to the Innovation fund Denmark for funding.

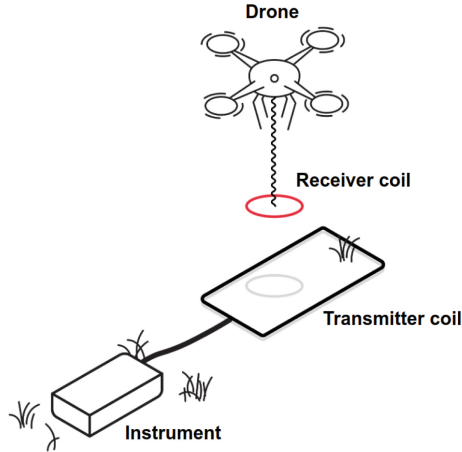


Fig. 1. The SuperTEM project involves three main technologies: an instrument for generating transmitter coil signals, a receiver coil for receiving these signals, and a drone to transport the receiver coil across the designated area.

transmitter and a drone-based receiver (Fig. 1). It aims to create a suspended load system for high-density data collection, although receiver motion may affect imaging accuracy and introduce electromagnetic noise. This paper will focus on modeling and creating the suspended slung load system.

Swing dampening has been researched for years because having a suspended load beneath a UAV affects the control adversely, thus making it difficult to operate accurately and efficiently and, in the worst case, leading to accidents. Therefore, different control strategies have been applied, such as in [4–6] where a feed-forward control system - based on input shaping - is used to reduce the oscillations by improving the damping of the swing of the slung load. In [4], a model-following control approach is employed to enhance the flight performance of a helicopter carrying a suspended load. Likewise, in [5], the helicopter and slung load system are constructed as a linear system on the state space form. This paper [7] proposes a modeling technique to address the issues of swing suppression and positioning control in a rigid-body model of a helicopter slung-load system under input constraints and external disturbances. The method utilizes Lagrange’s equations to establish the rigid-body model of the system. These studies [8,9] present a modeling and control approach for helicopter and slung-load systems. The approach in [8] employs physics-based models specifically designed for control applications, utilizing a point mass approach to model the dynamics of the external load. In [10–12], the authors create an overhead crane system model using a nonlinear dynamic model; this is rewritten to a state space representation. This author [13] focuses on creating a quadcopter and a cable-suspended load model with eight degrees of freedom. The focus is to create a trajectory that generates minimal load swing. In [14], the model and simulation of a fishing rod are constructed using Simscape in Simulink; additionally,

an elastic string is built using the lumped parameters method explained in the technical paper [15].

This paper contributes by creating a simulation model using off-the-shelf tools to test control design and path planning algorithms. The model focuses on visual aspects to enhance understanding of the system's behavior in the real world. The rest of the paper is organized as follows: Sect. 2 presents the method, model, and simulation strategy, Sect. 3 present several simulation results, and lastly, Sect. 4 discusses and concludes on the work presented.

2 Methodology

The slung load model consists of three parts: an attachment point, tethers, and the antenna, as seen in Fig. 2. Various methods can be used to model such a system, as stated in State of the art; however, this study has chosen to model the different parts as rigid bodies. Additionally, to make the tether flexible, the lumped-parameter method is used.

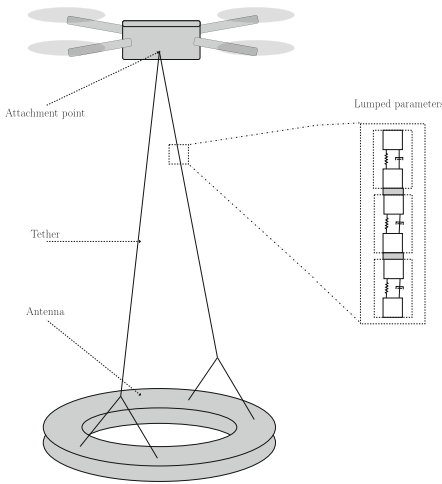


Fig. 2. The enlarged section illustrates that the tether is constructed using lumped parameters.

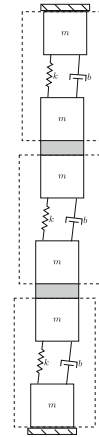


Fig. 3. A flexible body using the lumped-parameter method.

2.1 Lumped Parameters

The lumped parameters method approximates a flexible body by using a collection of discrete flexible units that are fixed together, as shown in Fig. 3. A unit is defined as two masses connected by a joint, where the joint is either translation or rotational. In addition, the degrees of freedom (DOF) of the joint determine the deformation of the element. Furthermore, the joint features internal springs

and dampers to describe the stiffness and damping between the bodies. Building a flexible body using the lumped parameters method requires four steps:

The first step is to model each mass element, illustrated as the block m in Fig. 3. Each mass corresponds to a mass element. These elements account for a small section of the body, where all the elements are assumed to be rigid. The accuracy of this method is depended on the number of elements used. Therefore, the model's accuracy tends to improve when the number of elements is increased; however, at the cost of computational time. The second step is to connect the mass elements in pairs with joints. These joints provide the DOF corresponding to different deformation types, e.g., translational movement enables axial deformation and shear, while rotational movement enables bending and torsion. The third step, springs and dampers are added to the joints between the masses, as illustrated in Fig. 3 with a spring and damper. They determine the static and dynamic deformation when forces and torques are applied to the joints. Therefore, coefficients for springs and dampers must be known or calculated from the material used. The fourth step is to rigidly connect each flexible body element to its neighbor, i.e., connecting the tether to the attachment point. To assemble it, rigid connections are added between each element.

2.2 Parameters

To calculate the drag on the antenna and tether, the second-order drag equation

$$D_l = \frac{1}{2} \rho C_d S_l |V|V \quad (1)$$

will be used, where ρ is the density of the air, C_d is the drag coefficient, S_l is the area, and V is the wind velocity relative to the object. The coefficient of drag is a function of the dimensionless ratio Reynolds number

$$Re = \frac{Vd}{v_i}, \quad (2)$$

where d is the diameter of the antenna and v_i is the viscosity of the air. From Reynolds number, the drag coefficient can be read from a graph with regard to the shape of the object.

2.3 Slung Load Model

Simulink has been used with a block library called Simscape, an application to Simulink, to construct a slung load system simulation model. It enables the creation of physical models of different systems and 3D visualization of the system.

Mechanical blocks model a suspended slung load system comprising an attachment point, tether, and suspended load. The attachment point, shown in Fig. 4, includes a base, setup parameters, a prismatic joint, and a velocity controller. The base serves as the attachment point for the tethers. Setup parameters consist of global frame access, simulation-wide configuration, and solver settings.

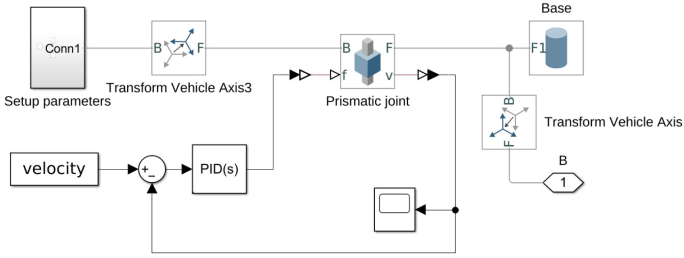


Fig. 4. Showing the different blocks used to build the attachment point.

The prismatic joint allows translational movement along an axis, with properties and control mechanisms configured within. A velocity block provides references for joint movement, controlled via PID controller. Transformation blocks handle rigid transformations between frames. Each tether element comprises various rigid blocks, as depicted in Fig. 5. The spherical joint provides three rotational degrees of freedom, allowing free rotation of one frame around another. Properties include state, actuation method, sensing, and internal mechanics like spring stiffness and damping.

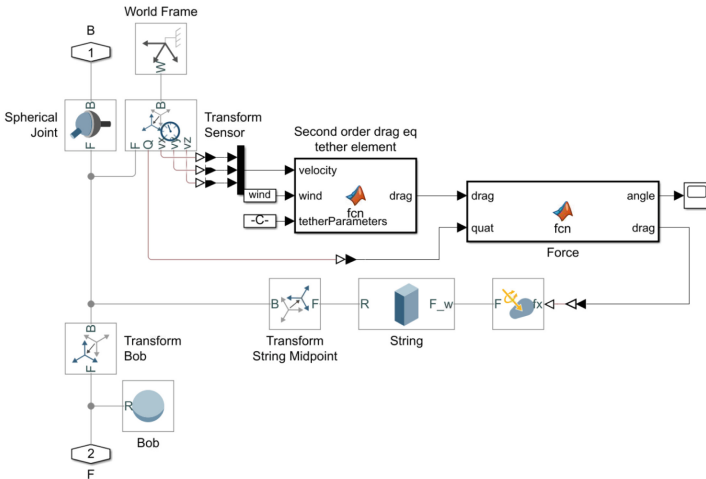


Fig. 5. Illustration of one string element.

The world frame and transform sensor are used to find the angle θ between the body frame of the string and the world frame. The two Matlab functions Second order drag eq tether element and Force are used to find the drag on the tether element. The second order drag eq tether element

3 Results

This section presents results from three simulations. The first explores variations in wind force on the tether and antenna, along with attachment point translation velocity, across three tests. The second simulation involves changing wind and translational velocities over an extended duration. The final simulation investigates the potential of using the lumped parameter method to induce tether bending when applying a force. Slung load parameters are listed in Table 1.

Table 1. Slung load parameters.

Parameters	Value	Unit
Single tether length	5	[m]
Split part of tether	1	[m]
Tether diameter	0.003	[m]
Weight of one meter tether	0.01	[kg]
Weight of Antenna	2.4	[kg]
Antenna height	0.1	[m]
Antenna outer radius	1.2	[m]
Antenna inner radius	1.1	[m]

Table 2. Reynolds numbers and drag coefficients for antenna and tether.

Parameters	Value
Antenna Re	4e+05
Tether Re	1000
Antenna C_d	0.4
Tether C_d	1.4

The optimal damping coefficient was determined through testing. A coefficient of 5 Nm/(rad/s) or lower results in loose tether oscillations without reaching steady state. Increasing the coefficient gradually damps oscillations, achieving stability at 20 Nm/(rad/s). Thus, 20 Nm/(rad/s) was chosen as the damping coefficient for the joints. Additionally, the spring constant in the joints was set to zero to minimize any spring effect in the tether. Equation 2 calculates Reynolds numbers for the antenna and tether, shown in Table 2. These values determine the drag coefficient by referencing a cylinder graph [16]. Both wind and translation velocity are selected based on expected conditions at the airfield.

In Fig. 7, an illustration of the slung load system is shown for the three tests, where the one denoted (a) is from the first test. In addition, in Fig. 8 a graph of the pitch angles of the antenna is shown for all three tests. Looking at the first test, where the only force is gravity, it is clear that the antenna, in a steady state, has an angle towards the ground at zero, which is expected when the only force is gravity. However, the graph shows that the antenna starts with a slight angle of -2° and settles at 0° . The system is not trimmed; therefore, it swings for 20–25 s before the slung load reaches a steady state.

In the second test, a wind force of 5 m/s is added. Figure 7b shows that the tethers are pushed slightly to the right compared to the previous Fig. 7a. The antenna angle is shown in the graph in Fig. 8. Compared to the first test, the fluctuation is greater at the beginning due to the wind added; however, steady state is reached at a similar time. The gravity and the wind reach an equilibrium, where the forces balance out, resulting in an antenna angle of four degrees.

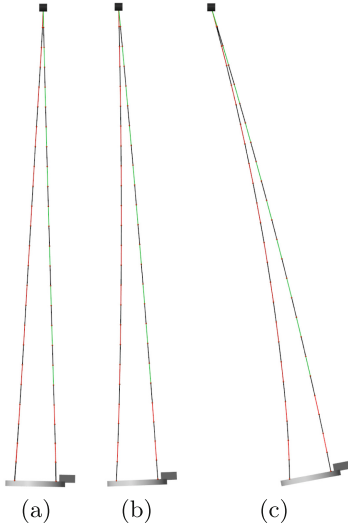


Fig. 7. Three test scenarios.

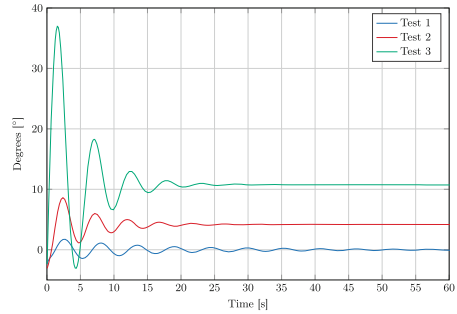


Fig. 8. The pitch angle of the antenna for the three tests.

The third test includes wind and translational movement of 5 m/s. The purpose is to observe the reaction of the slung load system to these factors. The results are presented in Figs. 7c and 8. In Figs. 7c, the wind (at 10 m/s) pushes the tethers and antenna further to the right compared to previous tests, indicating an increase in force. The graph shows a significant overshoot due to the fast acceleration of the attachment point, but it settles in approximately 20 s. The angle settles at 10.5° , more than double the previous test. Additionally, the bending of the tethers is observed, which is valuable for studying the impact of different tether configurations on slung load positioning under varying flight and wind conditions.

The next simulation shows how the slung load systems perform when subject to different translational and wind velocity inputs. The first subplot in Fig. 9 shows the pitch, roll, and yaw angle of the antenna, while the second subplot shows the input in translational and wind velocity. Steps one to three involve increasing translational velocity while keeping wind velocity constant. Step four varies wind velocity while keeping translational velocity constant. In step five, translational velocity is reduced. The difference in overshoot between translational and wind velocity steps is noticeable. Interestingly, the antenna angle reaches the same value at steady state in steps 3 and 5, indicating consistent force calculation on both antenna and tether. Additionally, both roll and yaw converge to zero after system initialization.

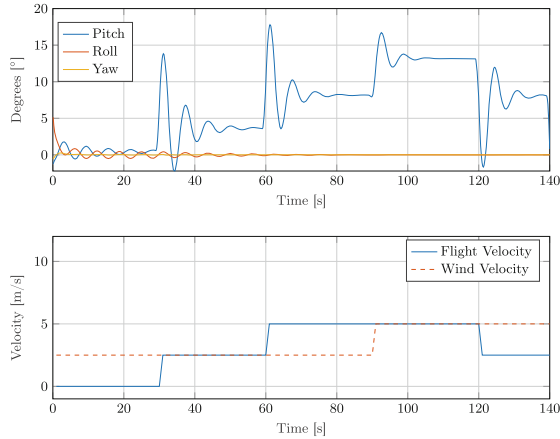


Fig. 9. The first subplot displays the antenna’s pitch, roll, and yaw angles, while the second subplot illustrates the various steps in flight and wind velocity.

4 Discussion and Conclusions

The model demonstrates the feasibility of creating a slung load model using the lumped parameter method and Simscape building blocks. This method offers versatility, allowing quick rearrangement of lumped parameters for different tether configurations while automatically updating 3D visualization. It provides valuable insights into slung load and tether behavior, aiding pilots in understanding potential challenges and making informed decisions for safe and efficient operations. Additionally, it can be used to develop control systems, such as input shaping or winch implementation, to optimize antenna positioning.

The choice of lumped parameters significantly impacts simulation time and model accuracy. Using 36 lumped parameters balances simulation speed and accuracy, making further testing and comparison with flight tests feasible. Compared to modeling with flexible beams in Simscape, the lumped parameter model is computationally less expensive due to fewer degrees of freedom and equations of motion. While the rigid body tether assumption simplifies modeling, it may not reflect real-world scenarios where tethers deform or stretch. This limitation underscores the need to carefully assess the model’s appropriateness and consider its assumptions and limitations when interpreting results. Future improvements could include replacing the Cartesian joint with a 6 DOF joint, allowing inputs from a drone model for more realistic movements and facilitating the development of control algorithms with similar dynamics to the physical system.

It can be concluded that a slung load model can be constructed in Simulink, with the help of the application Simscape and the lumped parameter method, and mimic the behavior of a slung load system. The next step is to compare this model to a physical system tested in similar conditions.

References

1. Auken, E., et al.: tTEM – a towed transient electromagnetic system for detailed 3D imaging of the top 70 m of the subsurface. *Geophysics* **84**(1), E13–E22 (2019)
2. Maurya, P.K., Christiansen, A.V., Pedersen, J., Auken, E.: High resolution 3D subsurface mapping using a towed transient electromagnetic system - tTEM: case studies. *Near Surface Geophys.* **18**(3), 249–59 (2020)
3. Christensen, N.B.: Joint inversion of airborne TEM data and surface geoelectrical data. The Egebjerg case. *J. Appl. Geophys.* **196**, 104511 (2022)
4. Adams, C., Potter, J., Singhose, W.: Input-shaping and model-following control of a helicopter carrying a suspended load. *J. Guid. Control. Dyn.* **38**(1), 94–105 (2015)
5. Bisgaard, M., la Cour-Harbo, A., Bendtsen, J.D.: Swing damping for helicopter slung load systems using delayed feedback. In: *Proceedings for AIAA Guidance Navigation and Control Conference* (2009)
6. Potter, J., Singhose, W., Costelloy, M.: Reducing swing of model helicopter sling load using input shaping. In: *IEEE International Conference on Control and Automation, ICCA*, pp. 348–53 (2011)
7. Ren, Y., Li, K., Ye, H.: Modeling and anti-swing control for a helicopter slung-load system. *Appl. Math. Comput.* **372**, 124990 (2020)
8. Oktay, T., Sultan, C.: Modeling and control of a helicopter slung-load system. *Aerosp. Sci. Technol.* **29**(1), 206–22 (2013)
9. Thanapalan, K., Zhang, F.: Modelling and simulation study of a helicopter with an external slung load system. *i-manager's J. Instrum. Control Eng.* **1**(1), 9-17 (2013)
10. Duc, T.H., Nguyen, H., Nguyen, Q.C.: Input shaping control of an overhead crane. In: *Vietnam Conference on Mechatronics* (2014). https://www.researchgate.net/publication/301619730_Input_shaping_Control_of_an_Overhead_Crane
11. Tumari, M.M., Shabudin, L., Zawawi, M.A., Shah, L.A.: Active sway control of a gantry crane using hybrid input shaping and PID control schemes. In: *IOP Conference Series: Materials Science and Engineering*, vol. 50, no. 1 (2013)
12. Hussien, S.Y.S., Ghazali, R., Jaafar, H.I., Soon, C.C.: The effects on sway angle performance in gantry crane system by using PSD analysis. *Jurnal Teknologi* **77**(21), 125–31 (2015)
13. Sreenath, K., Michael, N., Kumar, V.: Trajectory generation and control of a quadrotor with a cable-suspended load - a differentially-flat hybrid system. In: *Proceedings - IEEE International Conference on Robotics and Automation*, pp. 4888–4895 (2013)
14. Patra, S., Sarkhel, P., Hui, N.B., Banerjee, N.: Modelling and simulation of a fishing rod (flexible link) using simmechanics. *Journal European des Systemes Automatisés* **53**(4), 451–60 (2020)
15. Miller, S., Soares, T., Weddingen, Y.V., Wendlandt, J.: Modeling flexible bodies with Simscape multibody software. *Overview Two Methods Capturing Effects Small Elastic Deformations* (2016)
16. Brennen, C.: An internet book on fluid dynamics (2023). <http://brennen.caltech.edu/fluidbook/externalflows/drag/dragonasphere.pdf>



Research on Posture-Dependent Mode Coupling Chatter in Robotic Milling

Ming Ma¹, Xiong Huang¹, Tao Wu¹, Cencen Yang²(✉), and Lin Zhou²

¹ China Yangtze Power Co. Ltd., Wuhan, China

² The Wuhan Digital Design and Manufacturing Innovation Center Co. Ltd., Wuhan, China
yangcencen@niiddm.com

Abstract. In recent years, industrial robot has been widely used in milling because of its good flexibility. However, flexibility leads to the posture-dependent stability problem, while articulated structure makes mode coupling chatter more easily excited. All the above problems are research focus and difficulties in the robot milling field. In order to figure out the mechanism of posture-dependent mode coupling chatter in robotic milling, in this paper, a dynamic model considering the mode coupling chatter is first established, and the stability criterion of the mode coupling chatter is proposed by introducing the vibration form solution. Then the posture-dependence components in the stability criterion are derived in detail, the deformation ratio coefficient of the robot which refers to the ratio of vibration amplitude in different directions under the current cutting parameters is proposed, and the posture-dependence of the chatter is clarified. Finally, through simulation experiment, the change of robot stability with posture is analyzed, and the cutting experiment is used to verify the simulation results. The results show that the mode coupling chatter model of robot milling based on posture dependence is more accurate and can be used as the theoretical basis for the optimization of robot milling parameters such as posture optimization and tool path planning.

Keywords: Robotic Milling · Mode Coupling Chatter · Posture-dependent · Stability Prediction

1 Introduction

Because of its large working space and processing flexibility, industrial robots have been greatly promoted in milling in recent years [1]. However, due to its poor rigidity, there is an obvious coupling phenomenon between the degrees of freedom, that is, the force in a single direction will lead to deformation in three directions [2]. The phenomenon of displacement feedback will cause the mode coupling chatter, resulting in instability of the system [3, 4]. In addition, the hinge structure of the robot causes the pose dependence of the dynamic characteristics [5], which further increases the difficulty of predicting the mode coupling chatter of the robot. The accurate prediction of the mode coupling chatter of the posture-dependent robot milling is a hot and difficult point in the research of robot milling stability.

In order to address the aforementioned challenges, scholars around the world have conducted researches on robot chatter and posture-dependent frequency response prediction respectively [6–8]. In 2006, Pan et al. [9] established a mode coupling chatter dynamic model of the robot, decoupled it in the modal space, and finally judged its stability by solving the eigenvalue. In 2020, He et al. [10] developed a three-dimensional dynamic model for the robot's space milling plane, and obtained the corresponding stability criteria, and further obtained the mode-coupled flutter stability diagram, the experimental result verified that the model effectively prevents chatter by selecting a machining feed direction in stable region. In 2017, Cen et al. [11] considered the stiffness additional term brought by the external load in the robot stiffness model, and based on this, the mode coupling model was improved. The improved model can play the role of mode coupling chatter suppression without altering the direction of tool feed or the orientation of the workpiece. In 2019, Liu et al. [12] carried out reliability modeling based on the mode coupling chatter model of robot milling, and analyzed the influence of various parameters on the mode coupling chatter of robot. Huynh et al. [13] used a combination of multi-input and multi-output identification, computer-aided design model and experimental modal analysis to predict the dynamic characteristics of posture-dependent robots. In 2017, Yan et al. [14] based on the RCSA method of binary tree, quickly predicted the frequency response of the end tool tip of robot milling, and analyzed the stability of robot milling dependent on position and posture. In 2019, Celikag et al. [15] studied the dynamic characteristics of the robot under different postures, and proposed a machining strategy to suppress chatter by reconfiguring the joint angle during the machining process, which was verified by experiments. Similarly, in 2022, Chen et al. [16] introduced a novel method for estimating pose-dependent FRF at the TCP of machining robots by integrating data-driven (GPR) and physics-based (multibody dynamics) techniques, and the accuracy of this method was confirmed through impulse hammer tests.

At present, most of the research on the mode coupling chatter of posture-dependent robot milling is based on the posture-dependent robot frequency response prediction, and the model is too complicated and difficult to solve. In this paper, a dynamic model considering mode coupling chatter is first established. After that, in the derivation of the stability criterion, the stability criterion is simplified by using the vibration form solution, and the posture-dependent deformation ratio coefficient and its derivation process are presented in detail. The posture dependence is directly reflected in the stability criterion, which is simple in calculation and convenient for robot posture optimization or tool path planning. Finally, the robot milling stability verification experiment was carried out.

2 Stability Modeling Considering Modal Coupling

The weak rigid structure of the robot determines that it has obvious cross stiffness and cross damping characteristics. After applying force in a single direction, it will lead to deformation in three directions. Considering the cross frequency response

characteristics, the dynamic equation of the robot system is formulated as follows:

$$\begin{bmatrix} M_{xx} & M_{yx} & M_{zx} \\ M_{xy} & M_{yy} & M_{zy} \\ M_{xz} & M_{yz} & M_{zz} \end{bmatrix} \begin{bmatrix} \ddot{X}(t) \\ \ddot{Y}(t) \\ \ddot{Z}(t) \end{bmatrix} + \begin{bmatrix} C_{xx} & C_{yx} & C_{zx} \\ C_{xy} & C_{yy} & C_{zy} \\ C_{xz} & C_{yz} & C_{zz} \end{bmatrix} \begin{bmatrix} \dot{X}(t) \\ \dot{Y}(t) \\ \dot{Z}(t) \end{bmatrix} + \begin{bmatrix} K_{xx} & K_{yx} & K_{zx} \\ K_{xy} & K_{yy} & K_{zy} \\ K_{xz} & K_{yz} & K_{zz} \end{bmatrix} \begin{bmatrix} X(t) \\ Y(t) \\ Z(t) \end{bmatrix} = \begin{bmatrix} F_x(X, Y, Z) \\ F_y(X, Y, Z) \\ F_z(X, Y, Z) \end{bmatrix} \# \quad (1)$$

where M , C , K are the mass, damping and stiffness coefficients, respectively.

M_{ij} , C_{ij} , K_{ij} ($i, j = x, y, z$; $i \neq j$) represents the cross mass, cross damping and cross stiffness coefficient.

Due to the existence of modal coupling effect, the force in a single direction will be affected by multiple directions. Combined with the model of cutting force, considering the change of cutting force caused by displacement feedback, there is the following expression:

$$\begin{aligned} F_x + F'_x &= \sum_{j=1}^N g(\phi_j) \left(\begin{array}{l} Z'h(\phi_j) - Z'X(t) \cos \phi_j + Z'Y(t) \sin \phi_j - \\ Z(t)h(\phi_j) + Z(t)X(t) \cos \phi_j - Z(t)Y(t) \sin \phi_j \end{array} \right) K_{sx} \\ F_y + F'_y &= \sum_{j=1}^N g(\phi_j) \left(\begin{array}{l} Z'h(\phi_j) - Z'X(t) \cos \phi_j + Z'Y(t) \sin \phi_j - \\ Z(t)h(\phi_j) + Z(t)X(t) \cos \phi_j - Z(t)Y(t) \sin \phi_j \end{array} \right) K_{sy} \\ F_z + F'_z &= \sum_{j=1}^N g(\phi_j) \left(\begin{array}{l} Z'h(\phi_j) - Z'X(t) \cos \phi_j + Z'Y(t) \sin \phi_j - \\ Z(t)h(\phi_j) + Z(t)X(t) \cos \phi_j - Z(t)Y(t) \sin \phi_j \end{array} \right) K_{sz} \end{aligned} \quad (2)$$

Omit the second-order small quantity:

$$Z(t)X(t) \cos \phi_j - Z(t)Y(t) \sin \phi_j \approx 0 \# \quad (3)$$

where:

$$\begin{cases} F'_x = Z'h(\phi_j)K_{sx} \\ F'_y = Z'h(\phi_j)K_{sy} \\ F'_z = Z'h(\phi_j)K_{sz} \end{cases} \text{ and } \begin{cases} K_{sx} = -K_{tc} \sin \phi_j + K_{rc} \cos \phi_j \\ K_{sy} = -K_{tc} \cos \phi_j - K_{rc} \sin \phi_j \\ K_{sz} = K_{ac} \end{cases} \quad (4)$$

The force equilibrium position is taken as the initial position, so the cutting force caused by the axial cutting depth is not considered, and the final cutting force is expressed as:

$$\begin{aligned} F_x &= (-Z'X(t) \cos \phi_j + Z'Y(t) \sin \phi_j - Z(t)h(\phi_j))K_{sx} \\ F_y &= (-Z'X(t) \cos \phi_j + Z'Y(t) \sin \phi_j - Z(t)h(\phi_j))K_{sy} \\ F_z &= (-Z'X(t) \cos \phi_j + Z'Y(t) \sin \phi_j - Z(t)h(\phi_j))K_{sz} \end{aligned} \quad (5)$$

In robot milling, the structural rigidity of its own system is much lower than that of the workpiece. Therefore, compared with the deformation of the robot, the deformation of the workpiece part is often ignored. Therefore, this paper no longer considers the deformation of the workpiece part, and will use the established dynamic model of the

robot system and the cutting force model considering displacement feedback to derive the stability criterion.

The following will take the X direction as an example to derive the stability criterion.

By combining Eq. (5) and Eq. (1), and simplify, the following equation can be obtained:

$$\begin{aligned} & M_{xx}\ddot{X}(t) + C_{xx}\dot{X}(t) + (K_{xx} - Z' \cos \phi_j K_{sx})X(t) \\ & + M_{yx}\ddot{Y}(t) + C_{yx}\dot{Y}(t) + (K_{yx} + Z' \sin \phi_j K_{sx})Y(t) \\ & + M_{zx}\ddot{Z}(t) + C_{zx}\dot{Z}(t) + (K_{zx} + h(\phi_j)K_{sx})Z(t) = 0 \end{aligned} \quad (6)$$

Due to the displacement feedback effect, the stiffness coefficient of each degree of freedom is composed of two parts, namely the stiffness coefficient of the robot system itself and the displacement feedback coefficient. This is equivalent to changing the stiffness value of the robot system, and different forms of displacement feedback cause different types and degrees of change.

Let the vibration form solution of $X(t)$, $Y(t)$, $Z(t)$ be:

$$X(t) = A_X e^{pt}; Y(t) = A_Y e^{pt}; Z(t) = A_Z e^{pt} \quad (7)$$

By combining Eqs. (6) and (7), the subsequent equation can be derived:

$$\begin{aligned} & M_{xx}p^2 A_X e^{pt} + C_{xx}p A_X e^{pt} + K_{xx} A_X e^{pt} + M_{xy}p^2 A_Y e^{pt} + C_{yx}p A_Y e^{pt} \\ & + K_{yx} A_Y e^{pt} + M_{xz}p^2 A_Z e^{pt} + C_{zx}p A_Z e^{pt} + K_{zx} A_Z e^{pt} \\ & - Z' A_X e^{pt} \cos \phi_j K_{sx} + Z' A_Y e^{pt} \sin \phi_j K_{sx} - A_Z e^{pt} h(\phi_j) K_{sx} = 0 \end{aligned} \quad (8)$$

After rearranging the previous equation, we obtain:

$$\begin{aligned} & (M_{xx} + M_{yx} + M_{zx})p^2 + (C_{xx}A_X + C_{yx}A_Y + C_{zx}A_Z)p + K_{xx}A_X + K_{yx}A_Y \\ & + K_{zx}A_Z - (-Z'A_X \cos \phi_j K_{sx} + Z'A_Y \sin \phi_j K_{sx} - A_Z h(\phi_j) K_{sx}) = 0 \end{aligned} \quad (9)$$

If $p < 0$ in the equation, then the term in the solution of form converges to zero with time, the system is stable. On the contrary, it diverges with time and the system is unstable. Derived from the root formula:

$$\begin{aligned} a &= M_{xx}A_X + M_{yx}A_Y + M_{zx}A_Z \\ b &= C_{xx}A_X + C_{yx}A_Y + C_{zx}A_Z \\ c &= K_{xx}A_X + K_{yx}A_Y + K_{zx}A_Z - \begin{pmatrix} -Z'A_X \cos \phi_j K_{sx} \\ +Z'A_Y \sin \phi_j K_{sx} - A_Z h(\phi_j) K_{sx} \end{pmatrix} \end{aligned} \quad (10)$$

where a , b is always greater than zero. When:

$$\frac{-b \pm \sqrt{b^2 - 4ac}}{2a} < 0 \quad (11)$$

The system is stable, where $4ac > 0$, which means $c > 0$. The stability criterion is as follows:

$$\begin{aligned} & K_{xx}A_X + K_{yx}A_Y + K_{zx}A_Z > -Z'A_X \cos \phi_j K_{sx} \\ & + Z'A_Y \sin \phi_j K_{sx} - A_Z h(\phi_j) K_{sx} \end{aligned} \quad (12)$$